

Azimuthal-angle and energy distributions of Al^{2+} ejected from $\text{Al}(100)$ by Ar^+ bombardment

S. A. Larson and L. L. Lauderback*

Department of Chemical Engineering, University of Colorado, Boulder, Colorado 80309-0424

(Received 16 May 1990)

Azimuthal-angle and energy distributions of Al^{2+} ions ejected from an $\text{Al}(100)$ surface by Ar^+ bombardment have been measured and compared with corresponding measurements for Al^+ . Like the Al^+ angle distribution, the Al^{2+} azimuthal-angle distribution is generally quite anisotropic and reflects the fourfold symmetry of the $\text{Al}(100)$ surface. However, the Al^{2+} angle distribution generally exhibits a much stronger azimuthal anisotropy and a much stronger sensitivity to the kinetic energy of the ejected particles than does the Al^+ angle distribution. For Al^{2+} kinetic energies below ~ 55 eV, the intensity extrema in the Al^{2+} angle distribution occur at the same azimuthal angles as the extrema in the Al^+ angle distribution. However, the positions of the intensity extrema in the Al^{2+} angle distribution shift by 45° as the kinetic energy of the Al^{2+} ions increases from below 55 to above 55 eV, while the positions of the extrema in the Al^+ angle distribution are independent of energy. Preliminary molecular-dynamics simulations of the ejection process suggest possible Al^{2+} ejection mechanisms that are in accord with the observed angle and energy distributions. These mechanisms are consistent with the concept that Al^{2+} forms by de-excitation of $2p$ holes created by energetic Al-Al collisions in the solid.

INTRODUCTION

The translational angle distributions of neutral and singly charged ionic species ejected from ordered surfaces by ion bombardment have been shown to be a sensitive measure of the local geometric arrangement of surface atoms.¹⁻⁸ Correlations of measured neutral and ion angle distributions with molecular-dynamics simulations of the ejection process indicate that this structure sensitivity results from the tendency for particles to preferentially eject in directions between neighboring atoms where their ejection path is least obstructed.¹⁻⁸ For example, the azimuthal angle distributions of neutral and singly ionized metal atoms ejected from ordered metallic surfaces typically exhibit maxima in the directions of the open spaces between the surrounding nearest-neighbor atoms.¹⁻⁸ Such angle distributions thereby directly reflect the local geometric arrangement of the nearest-neighbor atoms of the original surface. For similar reasons, azimuthal angle distributions of singly charged atomic adsorbates ejected from ordered substrates have been found to be sensitive to their bonding site locations, both with respect to registry with the substrate and with respect to distance above or below the substrate surface.^{1-3,6-8} Recent studies also indicate that the polar angle distribution of ejected atomic adsorbates can be sensitive to their population in surface, subsurface, and defect sites on ordered substrates.⁸

In this paper we present what we believe are the first angle- and energy-resolved measurements of the azimuthal angle and energy distributions of doubly charged Al^{2+} ions ejected from a clean $\text{Al}(100)$ surface by Ar^+ bombardment. These measurements are compared with corresponding measurements of the azimuthal angle and energy distributions of ejected Al^+ ions in order to exam-

ine how the different ionization mechanisms responsible for emission of Al^+ and Al^{2+} influence the angle and energy distributions of these ions.

The ionization mechanism responsible for emission of Al^{2+} is believed to be considerably different from that responsible for emission of Al^+ . This is reflected, in part, from previous measurements of the Al^{2+} -to- Al^+ intensity ratio as a function of the primary ion energy. Such measurements involving polycrystalline Al foils⁹ have shown that the yield of Al^{2+} decreases much more rapidly than that of Al^+ as the primary ion energy decreases below ~ 5 keV and that the onset of emission of Al^{2+} requires a much higher primary ion energy than does the onset of Al^+ emission. The yield of Al^{2+} as a function of the primary ion energy has also been shown to correlate strongly with Auger electron and x-ray emissions.¹⁰⁻¹² These results have been interpreted as indicating that Al^{2+} ions are probably formed by violent collisions that produce Al $2p$ core level vacancies which subsequently decay by Auger deexcitation to produce the doubly charged Al^{2+} ions.¹⁰⁻¹² Analysis of electron correlation diagrams and recent measurements of Auger electron emission by ion bombardment of Al surfaces^{13,14} indicate that for Ar^+ bombardment, as used in this work, $2p$ vacancies are most likely created by symmetric Al-Al collisions as opposed to asymmetric Ar^+ -Al collisions. By contrast, Al^+ formation is believed to involve valence shell ionization by a "surface effect" such as resonant tunneling of a valence electron from the ejecting atom to an empty level in the surface.¹⁵ The formation of Al^+ is thus expected to be much less dependent on highly energetic Al-Al collisions than is the formation of Al^{2+} .

Since the dynamics of ejection of atomic species from solid surfaces is governed primarily by the dynamics of momentum transfer between colliding atoms, we expect

that any differences in the Al-Al collisional energies required to produce Al^+ and Al^{2+} will produce differences in the angle and energy distributions of ejected Al^+ and Al^{2+} . Our results show that substantial differences do in fact exist between the angle and energy distributions of ejected Al^+ and Al^{2+} ions. Preliminary molecular-dynamics simulations of the ejection process suggest possible ejection mechanisms that appear to be consistent with our observed angle and energy distributions. These mechanisms also appear to be consistent with the requirement of high energy Al-Al collisions in the Al^{2+} formation process.

EXPERIMENT

The angle resolved secondary ion mass spectrometry (ARSIMS) measurements were performed in a two-level turbomolecular-pumped stainless steel UHV chamber (base pressure = 5×10^{-10} torr) that is also equipped with Auger electron spectroscopy (AES), low-energy electron diffraction (LEED), and thermal desorption spectroscopy techniques. The primary Ar^+ ion beam used in the ARSIMS measurements was generated by a Coultron model G-2 ion gun and was mass analyzed by a Wien velocity filter. All experiments were performed with 4.5-keV Ar^+ ions impinging on the sample at normal incidence and with a current density of 5×10^{-8} Ams/cm². The primary ion beam was collimated to a diameter of 2.4 mm by a grounded aperture located ~ 3 cm in front of the sample. Secondary ions emitted from the sample surface were accepted into a Bessel box energy analyzer through an entrance aperture located in a grounded shield placed around the end of the energy analyzer. After passing through the energy analyzer, the secondary ions were subsequently mass analyzed by an Extranuclear Laboratories quadrupole mass spectrometer and detected using pulse counting techniques.

The azimuthal angle (ϕ) of the detected secondary ions could be varied from 0 to 180 degrees by rotating the crystal about its surface normal. The azimuthal angle is defined relative to the crystal orientation, as determined by LEED, in Fig. 1. All reported azimuthal angle distri-

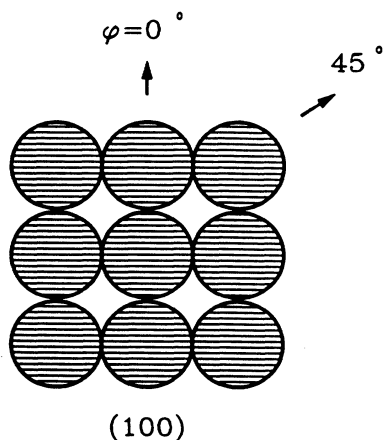


FIG. 1. Definition of the azimuthal orientation of the Al(100) plane.

butions were obtained at a fixed polar angle of 45 degrees, as measured from the surface normal, by measuring the Al^+ or Al^{2+} signal intensity at discrete 10-degree intervals from 0 to 180 degrees. From the sample position and aperture sizes, we estimate the angular resolution to be $\sim 7^\circ$.

The Al(100) crystal was obtained preoriented and pre-cut from the Monocrystals Company (99.999% purity) and was subsequently mechanically polished using standard techniques. The crystal was mounted on a sample holder via two stainless-steel clips. A chromel-alumel thermocouple was attached to one mounting clip for monitoring the sample temperature. Heating was accomplished by electron bombardment from behind the sample. The surface cleaning procedure consisted of many cycles of annealing to 450 °C and ion bombardment. Surface cleanliness and orientation were verified by AES and LEED, respectively.

RESULTS AND DISCUSSION

Before describing measurements of the azimuthal angle and energy distributions of the Al^+ and Al^{2+} secondary ions, we first show in Fig. 2, the variation of the Al^{2+} -to- Al^+ secondary-ion intensity ratio as a function of the primary Ar^+ ion energy. The values plotted in Fig. 2 correspond to 7.5-eV Al^+ and 15.0-eV Al^{2+} ion intensities averaged over azimuthal angles from $\phi=0^\circ$ to 180° . In agreement with previous studies involving polycrystalline Al(9), the Al^{2+} -to- Al^+ intensity ratio is seen to decrease rapidly with decreasing primary ion energy. Emission of Al^{2+} nearly ceases altogether for primary ion energies below ~ 2 keV. This result suggests that emission of Al^{2+} from Al(100) probably requires much higher collisional energies than does emission of Al^+ . This is in accord with the concept, described above, that emission of Al^{2+} involves the formation of Al $2p$ core level holes by violent Al-Al collisions whereas Al^+ formation occurs by

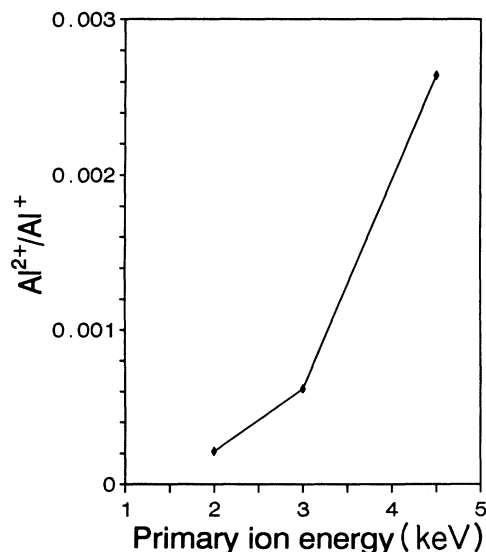


FIG. 2. Al^{2+} -to- Al^+ intensity ratio vs the Ar^+ primary ion energy. (See text for a description of experimental conditions.)

a valence ionization process. In the sections that follow we describe measurements of the azimuthal angle and energy distributions of the Al^+ and Al^{2+} secondary ions and examine how these distributions are influenced by the different ionization mechanisms involved in Al^+ and Al^{2+} emission process.

Angle distributions

The azimuthal angle distributions of the Al^+ and Al^{2+} ions that ejected from the $\text{Al}(100)$ surface with kinetic energies of 7.5 ± 3 and 15 ± 3 eV, respectively, are shown in Fig. 3. The intensity variations in this figure are plotted relative to the minimum intensity for each angle distribution. The fourfold symmetry of the $\text{Al}(100)$ surface is clearly reflected by the angle distribution of both ions which exhibit intensity maxima at $\phi = 45^\circ$ and 135° and minima at $\phi = 0^\circ$, 90° , and 180° . Comparison of the angle distributions with the crystal orientation, illustrated in Fig. 1, shows that the preferred ejection angles ($\phi = 45^\circ$ and 135°), for both Al^+ and Al^{2+} correspond to ejection in the directions of the open spaces between surrounding nearest-neighbor Al atoms on the original surface. However, while the angle distributions of Al^+ and Al^{2+} ex-

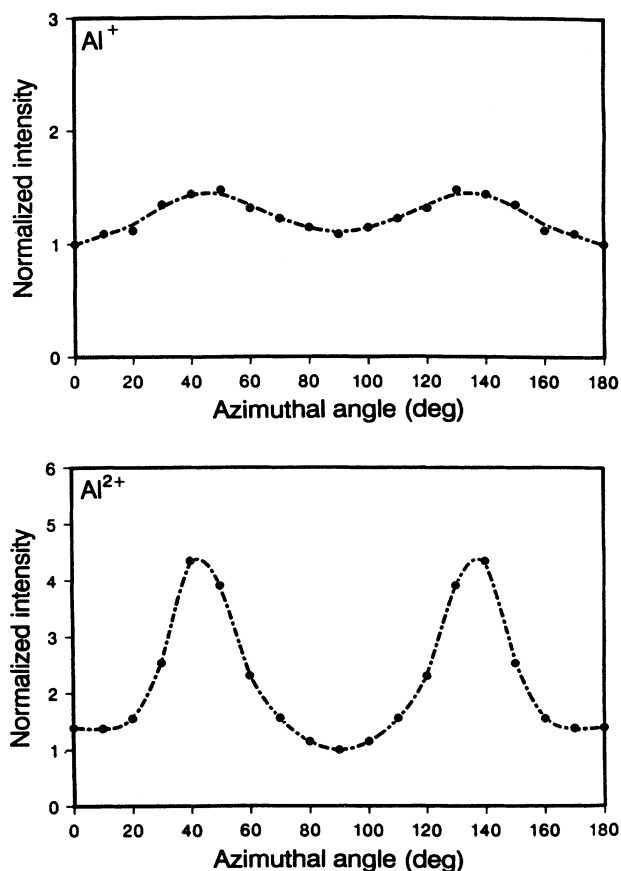


FIG. 3. Azimuthal angle distributions of Al^+ and Al^{2+} ejected from $\text{Al}(100)$ at kinetic energies of 7.5 ± 3 and 15.0 ± 3 eV, respectively.

hibit maxima and minima at the same azimuthal angles, the angular anisotropy of Al^{2+} is seen to be considerably greater than that for Al^+ . For the angular anisotropy defined as the ratio of the maximum to minimum intensity for each angle distribution, the azimuthal anisotropy of Al^+ is ~ 1.4 while that for Al^{2+} is ~ 4.4 .

The preference for Al^+ to eject in the directions between surrounding nearest-neighbor atoms is in agreement with previous ARSIMS measurements and with computer simulations of metal atom ejection from ordered metal surfaces.¹⁻⁸ The computer simulations show that metal atoms preferentially eject in the directions between nearest-neighbor atoms simply because their ejection path is least obstructed in these directions. Ejection directly toward nearest-neighbor atoms, on the other hand, is often blocked by strong repulsive scattering. The azimuthal angle distribution of Al^+ , therefore, reflects the local geometric arrangement of the nearest-neighbor atoms of the original surface directly through the influence of scattering interactions between the ejecting atom and its nearest neighbors. The fourfold symmetry of the Al^{2+} angle distribution and the direct correspondence of the angular positions of the peak maxima and minima of the Al^{2+} angle distribution to that for the Al^+ angle distribution suggest that the ejection dynamics of Al^{2+} is also sensitive to the geometric structure of the surface and might be influenced by the geometric arrangement of nearest-neighbor surface atoms in a manner similar to that for Al^+ . However, the much stronger angular anisotropy exhibited by Al^{2+} also suggests that details of the ejection mechanisms responsible for the structure sensitive ejection dynamics of Al^{2+} are at least somewhat different from those for Al^+ . Preliminary molecular dynamics simulations of the ejection process, described below, suggest that these apparent differences in ejection mechanisms relate directly to the requirement of high-energy Al-Al collisions in the formation of Al^{2+} .

Differences in the ejection dynamics of Al^+ and Al^{2+} become more dramatic as their kinetic energy increases. The azimuthal angle distributions of the Al^+ and Al^{2+} ions that ejected with kinetic energies of 35 ± 3 and 75 ± 3 eV, respectively, are shown in Fig. 4. Here it is seen that while both the Al^+ and Al^{2+} angle distributions still reflect the fourfold symmetry of the $\text{Al}(100)$ surface, the maximum and minimum intensities of the Al^+ and Al^{2+} angle distributions no longer occur at the same angular positions, but are shifted 45° out of phase from each other. In the case of the Al^+ angle distribution, the positions of the maxima and minima remain unchanged as the Al^+ kinetic energy increases from 7.5 (Fig. 3) to 35 eV. This reflects the tendency for both 7.5- and 35-eV Al^+ ions to be channeled in the directions of the open spaces between nearest-neighbor atoms as described above. The anisotropy of the Al^+ angle distribution is however, seen to increase somewhat from 1.4 at 7.5 eV to 1.7 at 35 eV. Such enhancement of the angular anisotropy with increasing kinetic energy has been observed in previous measurements and is predicted by molecular-dynamics simulations.^{2,3,5,6} The molecular-dynamics simulations show that this effect of kinetic energy results

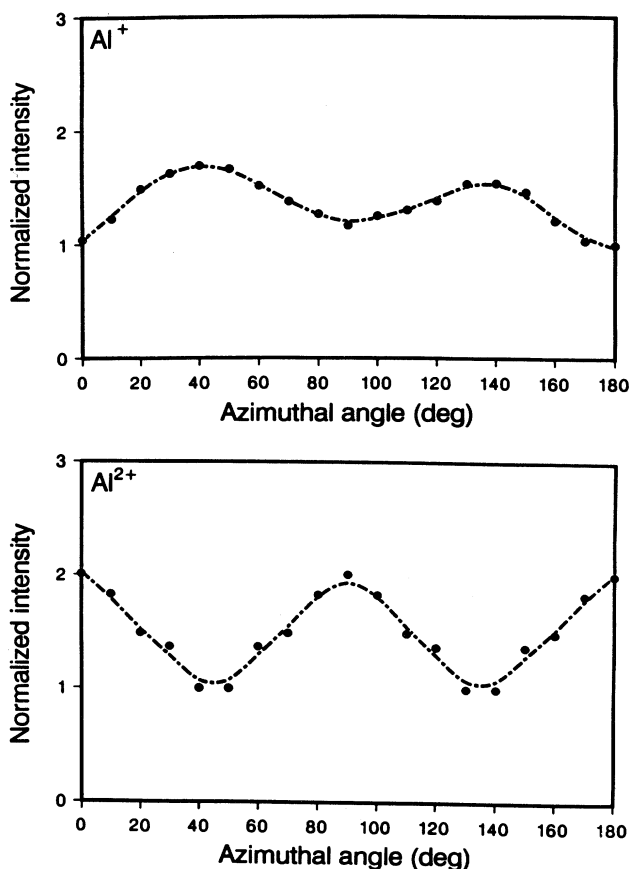


FIG. 4. Azimuthal angle distributions of Al^+ and Al^{2+} ejected from $\text{Al}(100)$ at kinetic energies of 35 ± 3 and 75 ± 3 eV, respectively.

from the fact that the lower energy ions tend to eject relatively late in the collision process after much of the original surface order responsible for the preferred ejection channels has been destroyed.

On the other hand, when the kinetic energy of the Al^{2+} ions increases from 15 eV (Fig. 3) to 75 eV, the angular positions of the maximum and minimum intensities of the Al^{2+} ions dramatically shifts by 45° . Thus, the 75-eV Al^{2+} ions preferentially eject in the azimuthal directions of the nearest-neighbor atoms ($\phi = 0^\circ, 90^\circ, 180^\circ$) instead of in the directions between neighboring atoms. This result indicates that the ejection mechanisms that govern the angle distribution of the 75-eV Al^{2+} ions are fundamentally different from those that govern the angle distribution of 15-eV Al^{2+} ions and the Al^+ ions. The fourfold symmetry of the angle distribution of the 75-eV Al^{2+} ions does indicate, however, that the ejection dynamics of the 75-eV Al^{2+} ions, while different from that for the 15-eV Al^{2+} and Al^+ ions, is still influenced by the crystal structure.

Additional insight into the different processes that govern the ejection dynamics of Al^+ and Al^{2+} at different secondary ion energies is obtained by examining the energy distributions of the ejected Al^+ and Al^{2+} ions.

Kinetic energy distributions

The kinetic energy distributions of the Al^+ and Al^{2+} ions that ejected at azimuthal angles of $\phi = 0^\circ$ and 45° are shown in Fig. 5. Both Al^+ energy distributions exhibit a single maximum at approximately 7–9 eV followed by a high energy tail that extends beyond 50 eV. The intensity of the Al^+ energy distribution for $\phi = 45^\circ$ is always greater than that for $\phi = 0^\circ$ at any given energy. This reflects the azimuthal anisotropy caused by the preference for Al^+ to eject in the directions between nearest-neighbor atoms. The Al^+ intensities at $\phi = 0$ and $\phi = 45^\circ$ do, however, vary somewhat relative to each other as the kinetic energy increases. This is seen in the upper panel of Fig. 6 which shows a plot of the Al^+ azimuthal anisotropy as a function of kinetic energy. At low kinetic energy, the Al^+ anisotropy increases with increasing energy. However, as the kinetic energy increases to higher values, the Al^+ anisotropy gradually levels off, reaching a maximum at about ~ 18 eV and subsequently decreases as the energy increases above 18 eV. As described above, the increase in the azimuthal anisotropy with increasing energy at low kinetic energies reflects the tendency for the lower energy ions to eject relatively late in the collision process after much of the original surface order is destroyed. We believe that the decrease in anisotropy with increasing kinetic energy at the higher energies (> 18 eV) may be caused by lower scattering cross sections of the

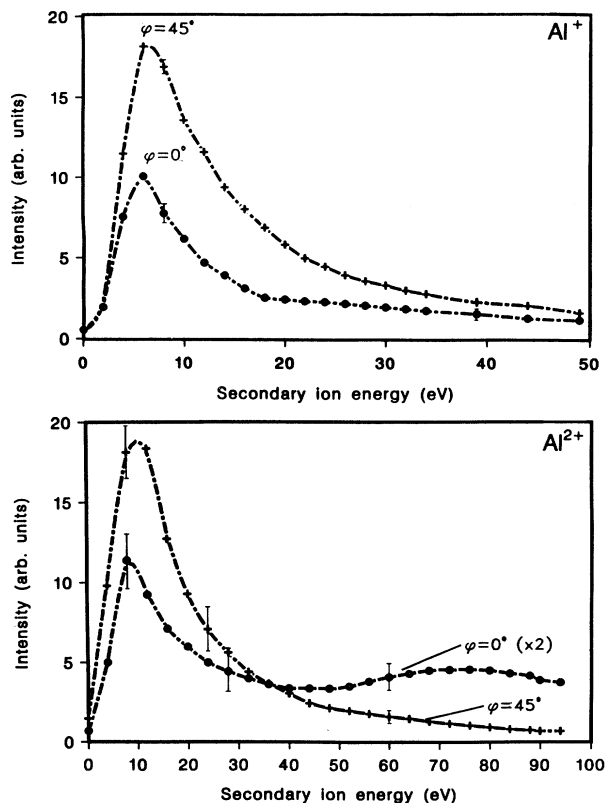


FIG. 5. Kinetic energy distributions of Al^+ and Al^{2+} ejected from $\text{Al}(100)$ at $\phi = 0^\circ$ and 45° .

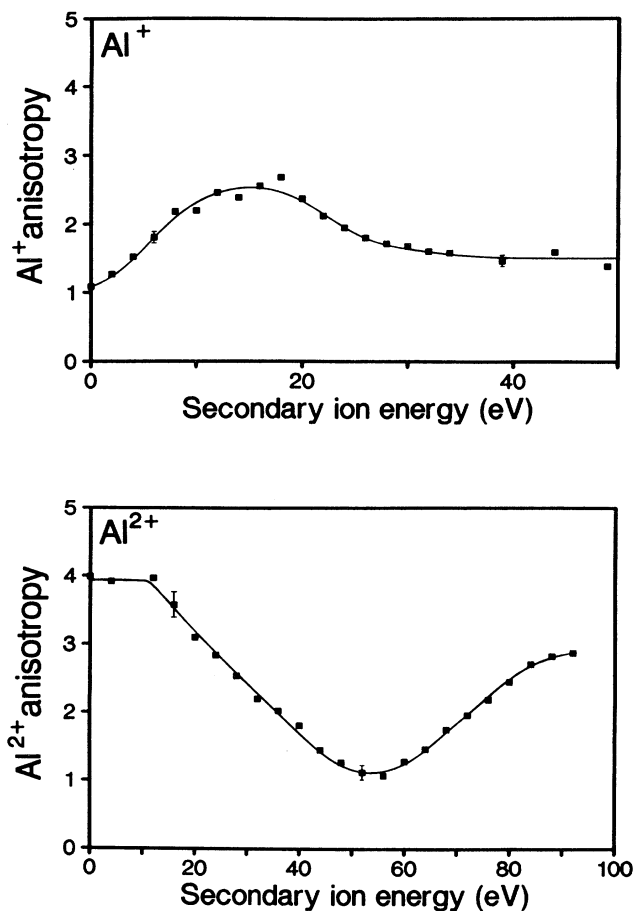


FIG. 6. Azimuthal anisotropy of Al^+ and Al^{2+} vs kinetic energy.

more energetic Al^+ ions, which effectively broadens the size of the ejection channels between nearest-neighbor atoms, and/or by a tendency for higher energy ions to deform the ejection channels.

The energy distributions of Al^{2+} (Fig. 5) exhibit a much stronger dependence on the azimuthal angle than those for Al^+ . While both Al^{2+} energy distributions for $\phi=0^\circ$ and 45° exhibit a low energy maximum near ~ 10 eV, a second broad peak centered at ~ 75 eV is observed only in the $\phi=0^\circ$ energy distribution. For kinetic energies below about ~ 30 eV, the Al^{2+} intensity at $\phi=45^\circ$ is considerably greater than that at $\phi=0^\circ$. This reflects the tendency for low energy Al^{2+} ions to preferentially eject at $\phi=45^\circ$ as indicated in Fig. 3. The shift in the angular positions of the intensity maxima and minima that occurs in the Al^{2+} angle distribution as the kinetic energy increases from 15 to 75 eV (see Figs. 3 and 4) is caused by the broad peak centered at 75 eV in the $\phi=0^\circ$ energy distribution. Apparently as the kinetic energy increases above roughly 30 eV, a new ejection mechanism is gradually “turned on” that selectively favors ejection at $\phi=0^\circ$, producing the broad high-energy peak in the $\phi=0^\circ$ ener-

gy distribution and the shift in location of the intensity extreme in the azimuthal angle distribution.

The influence of this high energy ejection mechanism on the anisotropy of the Al^{2+} azimuthal angle distribution is illustrated in the lower panel of Fig. 6. Here it is seen that as the energy increases from 0 to ~ 15 eV, the anisotropy remains essentially constant reflecting the preferred ejection of the low energy Al^{2+} ions at $\phi=45^\circ$. The anisotropy then begins to decrease as the kinetic energy increases above ~ 15 eV until it reaches a value of 1.0, corresponding to an isotropic distribution at ~ 55 eV. Measurements of the full angle distribution show that as the energy increases above 15 eV, the positions of the intensity maxima and minima remain fixed at $\phi=45^\circ$ and $\phi=0^\circ$, respectively, until the angle distribution becomes isotropic at ~ 55 eV. As the kinetic energy increases above 55 eV, the anisotropy increases again, but with the maximum and minimum intensities occurring at $\phi=0^\circ$ and $\phi=45^\circ$, respectively, as indicated in Fig. 4. It thus appears that the high-energy mechanism that favors ejection at $\phi=0^\circ$ first begins to influence the angle distribution at roughly 15–20 eV and dominates the preferred ejection angles for energies above ~ 55 eV.

Also of interest is the observation that at low energies (≤ 15 eV), the Al^{2+} anisotropy remains essentially constant instead of increasing with energy like the Al^+ anisotropy. This indicates that unlike Al^+ , the kinetic energy of ejected Al^{2+} is not strongly related to the degree of surface order at the time of ejection. We believe this is consistent with the concept that Al^{2+} ejection requires high-energy Al-Al collisions since such high-energy collisions are most likely to occur early in the collision process before the collisional energy is substantially dissipated and before the original surface order is significantly destroyed. Thus, most Al^{2+} ions probably eject early in the collision when the surface is still highly ordered regardless of their kinetic energy.

Finally, we note that while the maximum in the energy distributions of ejected Al^{2+} occurs at only ~ 10 eV (see Fig. 5), the minimum collisional energy (for a head on collision) required to reduce the internuclear Al-Al distance to the value necessary to induce $2p$ level ionization [about 0.65 \AA (Ref. 11)] is approximately 150 eV. Since the ionization potential for the $2p$ electron is only about ~ 78 eV,¹² the appearance of the maximum in the Al^{2+} energy distributions at only 10 eV suggests that if Al^{2+} forms by a collision induced $2p$ ionization process, the mechanism responsible for ejection of these low energy ions must involve substantial dissipation of the Al-Al collisional energy following the $2p$ ionization process. On the other hand, the processes responsible for the ejection of the high energy Al^{2+} ions that preferentially eject at $\phi=0^\circ$ apparently do not involve mechanisms for such extensive dissipation of energy following creation of the $2p$ hole. This information should provide a useful test of Al^{2+} ejection mechanisms that are proposed to account for the angle distributions of the low- and high-energy Al^{2+} ions. In the section that follows we examine possible Al^{2+} ejection mechanisms from analysis of molecular dynamics simulations of the Ar^+ -Al(100) collision process.

Molecular dynamics simulations

In an attempt to develop a deeper understanding of the events underlying the observed Al^{2+} angle and energy distributions, we have conducted preliminary classical molecular dynamics simulations of the Ar^+ -Al(100) collision process. The computational procedures used are the same as those described in a previous publications^{16–21} and will not be reviewed in detail here. The calculations were performed for 4-keV Ar^+ ions impinging at normal incidence onto the (100) surface plane of a model Al microcrystallite. The microcrystallite consisted of three atomic Al layers containing 88 atoms per layer. The interaction potential of the system was described by a sum of pair potentials between all atoms. The functional form of the pair potentials and the potential parameters are the same as those described in a previous publication.²²

Although the calculations do not account for ionization, we tested for possible Al^{2+} ejection mechanisms by selectively focusing on those mechanisms that involved symmetric Al-Al collisions of sufficient energy to form $2p$ core level vacancies (>150 eV). In this preliminary study, calculations were conducted for 100 Ar^+ impact points selected at random within an irreducible symmetry zone located near the center of the (100) crystal surface. For these 100 Ar^+ impacts only seven Al atoms were ejected by mechanisms involving Al-Al collisions of sufficient energy to create a $2p$ core hole. While this number is insufficient for predicting angle and energy distributions, it is of interest that all seven Al particles were ejected by only two very similar mechanisms which appear to account for the observed Al^{2+} angle and energy distributions shown in Figs. 3, 4, and 5.

These mechanisms are illustrated schematically in Fig. 7. In both mechanisms (a and b in Fig. 7), the incident Ar^+ ion collides with target atom 1 at such a point that target atom 1 is driven towards atom 2 in the second layer. A collision between atoms 1 and 2 then deflects atom 1 so it travels beneath the plane of the surface Al layer and between parallel rows of surface Al atoms that run in the $\phi=45^\circ$ direction. At this point, atom 1 is effectively channeled more or less along the $\phi=45^\circ$ azimuthal direction by the parallel rows of surface atoms and typically has a kinetic energy of 200–300 eV. Eventually, atom 1 encounters another second layer atom, atom 3. The energy of this collision is sufficient to form a $2p$ hole in either atom 1 or atom 3. Assuming a $2p$ hole forms in atom 1, two mechanisms can lead to ejection of Al^{2+} depending on the geometry of the atom-1–atom-3 collision.

In the first mechanism (mechanism a in Fig. 7) which accounted for six of the seven ejected Al atoms, atom 1 is deflected upward after colliding with atom 3 and collides with the surface atom 4. Atom 4 is then ejected on average in approximately the 45° azimuthal direction. The energy involved in the collision between atoms 1 and 4 is very low compared to that required for direct promotion of a $2p$ electron from atom 4 to the vacuum level and atom 4 typically ejects with a kinetic energy of only a few eV. We suggest, however, that since atom 1 contains a $2p$ hole as a result of its collision with atom 3, a resonant

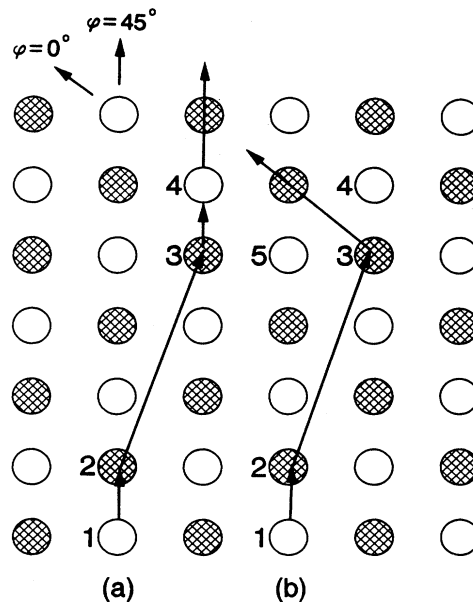


FIG. 7. Schematic of Al^{2+} ejection mechanisms predicted by molecular dynamics simulations, open circles represent surface Al atoms; crosshatched circles represent Al atoms in the second layer.

transition can occur that shifts the $2p$ vacancy from atom 1 to atom 4 during the atoms 1-4 collision. Atom 4 can then ionize above the surface by Auger deexcitation to form Al^{2+} . Alternatively, atom 4 can be doubly ionized by direct Auger deexcitation of the $2p$ vacancy in atom 1 during the collision. In either case, this mechanism is consistent with the concept that the Al^{2+} ions that preferentially eject at $\phi=45^\circ$ require violent Al-Al collisions and yet eject with relatively low kinetic energies (a few eV). This ejection mechanism also accounts for the large angular anisotropy of the low energy Al^{2+} ions on the basis of two principle factors: the first results from the channeling of atom 1 in the $\phi=45^\circ$ direction. This causes the momentum transferred from atom 1 to the ejecting atom 4 to also preferentially be directed in the $\phi=45^\circ$ direction, thus causing atom 4 to preferentially eject in the $\phi=45^\circ$ direction. In addition, the location of the nearest-neighbor surface atoms surrounding the ejecting atom 4 will also tend to channel the ejecting atom in the $\phi=45^\circ$ direction. We suggest that these effects of directed momentum transfer and channeling can combine to produce the much stronger azimuthal anisotropy observed for the low energy Al^{2+} ions relative to that for the Al^+ ions.

In the second mechanism that leads to possible ejection of Al^{2+} (mechanism b, Fig. 7) atom 1 is scattered upward in roughly the 0° azimuthal direction after colliding with atom 3. Atom 1 then travels between surface atoms 4 and 5 before ejecting. The kinetic energy of the ejecting atom in this mechanism is relatively large (~ 60 eV) since ejection occurs directly following the energetic atom-1–atom-3 collision responsible for the $2p$ core-hole formation rather than after a less energetic collision, as oc-

curred in the first mechanism (mechanism *a*). This mechanism favors ejection in the $\phi=0^\circ$ direction because of the tendency for the ejecting atom to be channeled between atoms 4 and 5. Particularly note that the position of atom 4 effectively blocks ejection of high energy Al^{2+} ions in the $\phi=45^\circ$ direction. This mechanism thus appears to be consistent with the observation that the high-energy Al^{2+} ions exhibit intensity maxima in the $\phi=0^\circ$, 90° , and 180° directions. Although definitive identification of the mechanisms responsible for the observed angle and energy distributions of ejected Al^{2+} will require further investigation, we believe it is significant that the mechanisms described here appear to account for the preferred ejection angles observed for both low- and high-energy Al^{2+} ions and are also consistent with the formation Al^{2+} by creation of $2p$ vacancies through energetic Al-Al collisions.

CONCLUSIONS

The azimuthal angle and energy distributions of Al^{2+} ions ejected from an Al(100) surface by Ar^+ bombardment have been measured and compared with the corresponding measurements for Al^+ . Like the Al^+ angle distribution, the Al^{2+} angle distribution is generally quite anisotropic and reflects the fourfold symmetry of the Al(100) surface. However, the Al^{2+} azimuthal angle distribution generally exhibits a much stronger anisotropy and has a much stronger dependence on the kinetic energy of the ejected ions than does the Al^+ azimuthal angle distribution. The low-energy Al^{2+} ions (< 30 eV) exhibit an azimuthal angle distribution with intensity maxima and minima in the same directions as the Al^+ ions (at $\phi=45^\circ$ and 135°) but with a much greater anisotropy. As the kinetic energy of the Al^{2+} ions increases above ~ 15

eV, however, the anisotropy of the Al^{2+} angle distribution begins to decrease due to a new Al^{2+} ejection mechanism that favors ejection of high-energy Al^{2+} ions in the $\phi=0^\circ$, 90° , and 180° directions. The influence of the mechanism favoring ejection at $\phi=0^\circ$, 90° , and 180° increases with increasing kinetic energy and dominates the preferred ejection angles of those Al^{2+} ions that eject with kinetic energies above 55 eV. The preferred ejection angles of Al^{2+} therefore change from $\phi=45^\circ$ and 135° for kinetic energies below ~ 55 eV to $\phi=0^\circ$, 90° , and 180° for Al^{2+} kinetic energies above 55 eV. The azimuthal angle distribution for the 55-eV Al^{2+} ions is essentially isotropic. The occurrence of the mechanism that favors ejection of the high-energy Al^{2+} ions at $\phi=0^\circ$, 90° , and 180° is also reflected by the appearance of a broad peak centered at ~ 75 eV in the energy distribution of the Al^{2+} ions that ejected at $\phi=0^\circ$. Preliminary molecular-dynamics simulations of the ejection process suggested possible ejection mechanisms that could account for the observed angle and energy distributions of the ejected Al^{2+} ions. The ejection mechanisms found to be consistent with the observed angle and energy distributions are in accord with the concept that Al^{2+} ejection requires violent Al-Al collisions of sufficient energy to produce Al $2p$ core holes.

ACKNOWLEDGMENTS

The authors wish to thank B. J. Garrison for supplying the computer code used for the molecular dynamics simulations. We gratefully acknowledge financial support of this work by the National Science Foundation (Grants No. CPE 8 307 303, CPE 8 305 341, and CPE 8 405 763).

*To whom correspondence should be addressed and present address: University of Nebraska-Lincoln, Department of Chemical Engineering, 236 Avery Laboratory, Lincoln, NE 68588-0126.

¹N. Winograd, B. J. Garrison, and D. E. Harrison, Jr., *Phys. Rev. Lett.* **41**, 1120 (1978).

²N. Winograd and B. J. Garrison, *Acc. Chem. Res.* **13**, 406 (1980).

³S. P. Holland, B. J. Garrison, and N. Winograd, *Phys. Rev. Lett.* **43**, 220 (1979).

⁴B. J. Garrison, C. T. Reimann, and N. Winograd, *Phys. Rev. B* **36**, 3516 (1987).

⁵R. A. Gibbs, S. P. Holland, K. E. Foley, B. J. Garrison, and N. Winograd, *J. Chem. Phys.* **76**, 684 (1982).

⁶W. N. Delgass, L. L. Lauderback, and D. G. Taylor, *Springer Series in Chem. Phys.* **20**, 51 (1981).

⁷L. L. Lauderback and S. A. Larson, in *Proceedings of the Tenth North American Meeting of the Catalysis Society*, edited by J. W. Ward (Elsevier, Amsterdam, 1987), p. 845.

⁸L. L. Lauderback and S. A. Larson (unpublished).

⁹D. Brochard and G. Slodzian, *J. Phys. (Paris)* **32**, 185 (1971).

¹⁰P. Joyes, *J. Phys.* **30**, 365 (1969).

¹¹P. Joyes, *Radiat. Eff.* **19**, 235 (1973).

¹²M. Barat and W. Lichten, *Phys. Rev. A* **6**, 211 (1972).

¹³P. Viaris de Lesegno, G. Rivais, and J. F. Hennequin, *Phys. Lett* **49A**, 265 (1974).

¹⁴J. F. Hennequin and P. Viaris de Lesegno, *Surf. Sci.* **42**, 50 (1974).

¹⁵P. Williams, *Surf. Sci.* **90**, 588 (1979).

¹⁶D. E. Harrison, Jr., W. L. Moore, Jr., and H. T. Holcombe, *Radiat. Eff.* **17**, 167 (1973).

¹⁷D. E. Harrison, Jr., P. W. Kelly, B. J. Garrison, and N. Winograd, *Surf. Sci.* **76**, 311 (1978).

¹⁸B. J. Garrison, N. Winograd, and D. E. Harrison, Jr., *J. Chem. Phys.* **69**, 1440 (1978).

¹⁹N. Winograd, D. E. Harrison, Jr., and B. J. Garrison, *Surf. Sci.* **78**, 6000 (1978).

²⁰B. J. Garrison, N. Winograd, and D. E. Harrison, Jr., *Phys. Rev. B* **18**, 6000 (1978).

²¹N. Winograd, B. J. Garrison, and D. E. Harrison, Jr., *J. Chem. Phys.* **73**, 3473 (1980).

²²L. L. Lauderback, A. J. Lynn, C. J. Waltman, and S. A. Larson, *Surf. Sci.* (to be published).